Nephron Progenitor But Not Stromal Progenitor Cells Give Rise to Wilms Tumors in Mouse Models with β-Catenin Activation or *Wt1* Ablation and *Igf2* Upregulation[1]

Le Huang*, Sharada Mokkapati‡, Qianghua Hu‡, E. Cristy Ruteshouser‡, M. John Hicks§,¶ and Vicki Huff*,†,‡,§

*Graduate Program in Genes and Development, The University of Texas Graduate School of Biomedical Sciences, Houston, TX 77030; †Graduate Program in Human and Molecular Genetics, The University of Texas Graduate School of Biomedical Sciences, Houston, TX 77030; ‡Department of Genetics, The University of Texas MD Anderson Cancer Center, Houston, TX 77030; §Department of Pathology, Texas Children's Hospital, Houston, TX 77030; ¶Department of Pathology, Immunology and Pediatrics, Baylor College of Medicine, Houston, TX 77030

Abstract

Wilms tumor, a common childhood tumor of the kidney, is thought to arise from undifferentiated renal mesenchyme. Variable tumor histology and the identification of tumor subsets displaying different gene expression profiles suggest that tumors may arise at different stages of mesenchyme differentiation and that this ontogenic variability impacts tumor pathology, biology, and clinical outcome. To test the tumorigenic potential of different cell types in the developing kidney, we used kidney progenitor-specific Cre recombinase alleles to introduce *Wt1* and *Ctnnb1* mutations, two alterations observed in Wilms tumor, into embryonic mouse kidney, with and without biallelic *Igf2* expression, another alteration that is observed in a majority of tumors. Use of a *Cre* allele that targets nephron progenitors to introduce a *Ctnnb1* mutation that stabilizes β-catenin resulted in the development of tumors with a predominant epithelial histology and a gene expression profile in which genes characteristic of early renal mesenchyme were not expressed. Nephron progenitors with *Wt1* ablation and *Igf2* biallelic expression were also tumorigenic but displayed a more triphasic histology and expressed early metanephric mesenchyme genes. In contrast, the targeting of these genetic alterations to stromal progenitors did not result in tumors. These data demonstrate that committed nephron progenitors can give rise to Wilms tumors and that committed stromal progenitors are less tumorigenic, suggesting that human Wilms tumors that display a predominantly stromal histology arise from mesenchyme before commitment to a stromal lineage.

Neoplasia (2016) 18, 71–81

Introduction

Wilms tumor is a kidney tumor diagnosed primarily in children under the age of five. It is an embryonal tumor and typically exhibits a triphasic histology comprised of cells at differing stages of differentiation that are normally seen in the developing kidney: blastemal cells similar to early, undifferentiated metanephric mesenchyme; epithelial cells arranged in disorganized duct-like structures very similar to nephron ductal epithelial cells; and stromal cells. During normal kidney development, each of these cell types arises from intermediate mesenchyme, and Wilms tumors are generally thought to arise from undifferentiated intermediate and metanephric mesenchyme. However, tumors are very heterogeneous histologically, which has led to the suggestion that variable tumor histology may be a result of mesenchymal cells being mutated and

transformed at different stages of mesenchymal differentiation. For example, some tumors display predominantly stromal or predominantly epithelial elements, raising the question of whether this distinct histology is the result of transformation of a cell already fated to become stromal or nephron epithelium, respectively.

The kidney is derived from *Osr1* expressing intermediate mesoderm [1]. A very small population of cells expressing both *Foxd1* and *Six2* is present at the onset of metanephric mesenchyme outgrowth and can transiently contribute to nephron epithelium fated cells [2,3]. Subsequently, two major types of progenitor populations exist: nephron progenitors and stromal progenitors [2,4–6]. Nephron progenitors give rise to the majority of the cells in the nephron. The undifferentiated and self-renewing population of uninduced nephron progenitors expresses *Cited1* and *Six2* [7]. Upon stimulation of BMP7-Smad signaling, these cells lose expression of *Cited1* but not *Six2* and become sensitive to Wnt9/β-catenin signaling from the ureteric bud, resulting in expression of *Wnt4* and *Lef1* and epithelialization [8]. In comparison, stromal progenitors specifically express *Foxd1* and give rise to the interstitium, pericytes, and mesangial cells [2,6]. Thus, triphasic Wilms tumors with blastemal (mesenchymal), epithelial, and stromal elements have been thought to arise before the specification of nephron or stromal progenitors. Similarly, stromal-predominant tumors have been proposed to originate from a stromal progenitor.

Gene expression analysis of a large panel of Wilms tumors resulted in the identification of five subsets of tumors which, in addition to their differing expression profile, displayed differing gene mutation frequencies, histologic features, and clinical outcomes [9]. From this work, a model of Wilms tumor ontogeny was proposed, but, to date, experimental data regarding the cellular ontogeny of Wilms tumor have been lacking.

We previously successfully generated a genetic endogenous tumor mouse model for Wilms tumor by somatically and mosaically introducing into fetal kidney a combination of alterations observed in human tumors: ablation of *Wt1*; a transcription factor essential for kidney development; and biallelic expression of *Igf2*, a fetal mitogen. This was accomplished by use of a ubiquitously expressing, tamoxifen-inducible transgene encoding Cre-recombinase. Tumors from these mice (*U-Cre-Wt1-Igf2*) recapitulated the classic triphasic histology of human tumors [10]. This experimental system now enables us to investigate whether mutations targeted to specific cellular compartments of the developing kidney are tumorigenic and, if so, whether the histology of tumors varies depending upon the differentiation status of the targeted cell.

Using *Cre* alleles expressed specifically in FOXD1$^+$, CITED1$^+$, and SIX2$^+$ cells to target stromal and nephron progenitors, respectively, we tested the tumorigenic effect of 1) *Wt1* ablation and *Igf2* biallelic expression and 2) *Wt1* ablation and *Ctnnb1* (β-catenin) stabilizing mutations, another combination of alterations observed in human Wilms tumors [11], in these two major compartments of the developing kidney. We found that, with these alterations, tumors developed from nephron progenitors but not stromal progenitors. Moreover, introduction of a stabilizing *Ctnnb1* mutation into nephron progenitors using both the *Cited1-Cre* (*Cited1^{Cre}*) and the *Six2-Cre* (*Six2^{GCE}*) alleles resulted in tumors irrespective of *Wt1* ablation. Of note, these tumors displayed an epithelial-predominant histology. In contrast, introduction of *Wt1*-ablation and *Igf2* biallelic expression (*Wt1-Igf2*) using the *Cited1^{Cre}* transgene was tumorigenic but not when the *Six2^{GCE}* allele was employed. These *Cited1^{Cre}-Wt1-Igf2* tumors displayed a triphasic histology. Thus, both the differentiation status of the targeted cell and the type of mutations introduced had a significant impact on tumorigenesis.

Materials and Methods

Mice

The *Foxd1^{GCE}* (B6;129S4-Foxd1$^{tm2(GFP/cre/ERT2)Amc}$/J), *Six2^{GCE}* (B6;129-Six2$^{tm3(EGFP/cre/ERT2)Amc}$/J), *Cited1^{Cre}* (Cited1-CreER^{TM}-GFP), *R26^{tdTomato}* (B6;129S6-Gt(ROSA)26Sor$^{tm14(CAG-tdTomato)Hze}$/J), *Ctnnb1$^{ex3(fl)}$*, *Wt1-* (B6.129S4-^{Wt1tm1Jae}/J), *Wt1^{fl}*, and *H19$^-$* mouse strains were used for these studies and have been described previously [5,6,12–17]. In the *Foxd1^{GCE}* and *Six2^{GCE}* strains, a GFP-Cre cassette is under the control of the endogenous *Foxd1* and *Six2* promoters, respectively, whereas the *Cited1-CreER^{TM}-GFP* strain is a BAC transgenic mouse line in which a GFP-Cre expression construct is under the control of a 190-kb genomic fragment 5' of the *Cited1* gene. For all three Cre lines, Cre-recombinase function is inducible in a dose-dependent manner by tamoxifen (TM), and embryos were treated *in utero* with TM by intraperitoneal injection of the pregnant female to induce Cre activity. Recombination of the *Ctnnb1$^{ex3(fl)}$* allele results in an in-frame deletion of exon 3 which stabilizes the resulting protein and activates the Wnt/β-catenin pathway [16]. Recombination of the *Wt1^{fl}* allele results in ablation of *Wt1* function [15]. The *H19$^-$* allele carries a deletion of H19 and the imprinting control region (ICR1) that is required for silencing of the maternal *Igf2* locus. Maternal inheritance of *H19$^-$* (*H19^{-m}*) results in biallelic expression of *Igf2* [17].

Mice were maintained on a C57BL/6 J × 129/SvEv mixed genetic background, housed in a pathogen-free environment, and handled according to the guidelines of The University of Texas MD Anderson Cancer Center Institutional and Animal Care and Use Committee. Overall, similar numbers of male and female mice were used.

Genotyping

Genotyping of mice (tail and normal tissue DNA) and tumors (tumor DNA) was carried out using previously described conditions [10].

Validation of Progenitor Cell-Type Specific Expression of Cre Alleles

To confirm the progenitor specificity of the different Cre alleles and to estimate the proportion of kidney cells resulting from progenitor-specific targeting, *Foxd1$^{GCE/+}$*, *Six2$^{GCE/+}$*, or *Cited1$^{Cre/+}$* mice were crossed with tdTomato reporter mice expressing the *loxP-Stop-loxP tdTomato* transgene (*R26^{tdTomato}*). *Cre$^+$; R26$^{tdTomato/+}$* embryos were treated with TM (1 or 3 mg/40 g body weight [BW]) at E11.5, E14.5, or E17.5. Embryonic kidneys were harvested at E19.5 and assessed by immunofluorescence (IF) histology. To estimate the frequency of Cre-mediated recombination, kidneys were also harvested at E14.5 and E19.5 and dissociated into single-cell suspensions which were sorted by fluorescence-activated cell sorting analysis (FACS) as described below.

Generation of Tumor-Watch Cohorts

To generate tumor-watch cohorts, *Cre$^+$; Wt1$^{+/-}$* males were bred with Wt1$^{fl/fl}$; *Ctnnb1$^{ex3(fl)/ex3(fl)}$* or *Wt1$^{fl/fl}$; H19$^{-/-}$* females to generate embryos with the following genotypes: 1) *Foxd1^{GCE}; Wt1$^{-/fl}$* or *Wt1$^{+/fl}$; Ctnnb1$^{+/ex3(fl)}$* (*F-Wt1-β-cat^S*), 2) *Foxd1^{GCE}; Wt1$^{-/fl}$; H19$^{+/-m}$* (*F-Wt1-Igf2*), 3) *Six2^{GCE}; Wt1$^{-/fl}$* or *Wt1$^{+/fl}$; Ctnnb1$^{+/ex3(fl)}$* (*S-Wt1-β-cat^S*), 4) *Six2^{GCE}; Wt1$^{-/fl}$; H19$^{+/-m}$* (*S-Wt1-Igf2*), 5) *Cited^{Cre}; Wt1$^{-/fl}$; Ctnnb1$^{+/ex3(fl)}$* (*C-Wt1-β-cat^S*), and 6) *Cited^{Cre}; Wt1$^{-/fl}$; H19$^{+/-m}$* (*C-Wt1-Igf2*). Embryos were treated by intraperitoneal injection of pregnant dames with TM (0.5, 1 or 3 mg/40 g BW) to induce Cre activity in specific fetal kidney progenitors. For *Foxd1^{GCE}*, TM was administered at E11.5. For *Six2^{GCE}*, TM was administered at E11.5 or E14.5. In addition to its

expression in fetal kidney nephron progenitors, $Cited1^{Cre}$ is expressed in fetal liver progenitors at E14.5, and β-catenin activation by $Cited1^{Cre}$ at E14.5 in the fetal liver led to the development of hepatocellular carcinoma at an early age in > 90% of mice [18]. Because of this competing phenotype, $C\text{-}Wt1\text{-}β\text{-}cat^{S}$ embryos were treated at E17.5, at which point $Cited1^{Cre}$ expression was undetectable in fetal liver [18] but still robust in fetal kidney. $Wt1$ ablation with $Cited1^{Cre}$ in the context of $Igf2$ biallelic expression following TM injection at E14.5 did not result in a detectable liver phenotype, and this time point was used to generate the $C\text{-}Wt1\text{-}Igf2$ cohort. Mutant mice and littermate controls were monitored for tumor development.

Histology and Immunohistochemistry

Tumor and kidney tissue specimens for hematoxylin and eosin (H&E) and immunohistochemistry (IHC) analyses were fixed in 4% paraformaldehyde, embedded in paraffin, and cut into 5-μm sections. Samples for IF staining were processed in ornithine carbamoyltransferase compound and cut into 12-μm frozen sections. H&E, IHC, and IF analyses of proteins were performed as described previously [10]. Antibodies used were: WT1 (sc-192, Santa Cruz Biotechnology), Ki67 (ab15580, Abcam), pHH3 (06-570, Upstate Biotechnology), β-catenin (610154, BD Biosciences), Dlk1 (sc-8624, Santa Cruz Biotechnology), Cited1 (9219, Fisher Scientific), Six2 (11562-1-AP, Proteintech), Pax2 (PRB-276P, Covance), NCAM (C9672, Sigma), E-cadherin (3195, Cell Signaling Technology), K-cadherin (ab79005, Abcam), Vimentin (V2258, Sigma), Collagen IV (AB756P, Chemicon), Cyclin D1 (sc-753, Santa Cruz Biotechnology), and C-myc (9E10, Santa Cruz Biotechnology).

Fluorescence-Activated Cell Sorting Analysis

Single-cell suspensions from fetal kidneys harvested at E15.5 or E19.5 from $Foxd1^{GCE/+}$; $R26^{tdTomato/+}$ embryos, $Six2^{GCE/+}$; $R26\text{-}^{tdTomato/+}$ embryos, and $Cited1^{Cre/+}$; $R26^{tdTomato/+}$ embryos were prepared as previously described [5]. Cells expressing tdTomato as a result of Cre-mediated recombination of the conditionally expressed tdTomato reporter were isolated with the BD FACS Aria high-speed digital cell sorter (BD Biosciences). Cell suspensions from littermate kidneys without a Cre allele served as negative controls.

Gene Expression Analysis

Tumor or kidney tissue was flash-frozen in liquid nitrogen. RNA was extracted from specimens or cell pellets using the RNA-queous-4PCR kit (Ambion) and converted to cDNA using reverse transcription reagents (Applied Biosystems). Real-time polymerase chain reaction (PCR) was performed using SYBR Green reagent with a 7900HT sequence detection system (Applied Biosystems) using transcript-specific primers (Supplementary Table 2).

Statistical Analysis

The Student t test or analysis of variance was used to analyze real-time PCR results. Results were presented as mean values with standard deviation. P values less than .05 were considered statistically significant.

Results

Validation of Progenitor Cell-Type Specific Expression of Cre Alleles

Lineage tracing of cells derived from targeted progenitors confirmed the specificity of the Cre alleles used (Figure 1A). As expected, use of the $Six2^{GCE}$ and $Cited1^{Cre}$ alleles resulted in

tdTomato expression in nephron progenitors and their daughter cells, e.g., comma-shaped bodies, S-shaped bodies, proximal tubules, distal tubules, and glomeruli. Also as expected, as the time between TM injection and harvesting the kidney increased, tdTomato expression shifted more medially as labeled progenitors differentiated and kidney development continued at the periphery. Use of the stromal progenitor-specific Cre ($Foxd1^{GCE}$) resulted in labeled stromal progenitors and their descendent cells. FACS analysis of kidney cell suspensions for tdTomato^{+} cells at E15.5 and E19.5 was also carried out. A representative FACS sorting plot is shown in Figure 1B. tdTomato^{+} cells represented 30% to 33% of total kidney cells following $Six2^{GCE}$-mediated recombination and 5% to 7% following recombination with either the $Cited1^{Cre}$ or $Foxd1^{GCE}$ alleles (Figure 1C and Table 1).

Targeting of Nephron, But Not Stromal, Progenitors Results in Wilms Tumor Development

As shown in Table 2, $Wt1^{-/fl}$; $Ctnnb1^{+/ex3(fl)}$ cohorts carrying either the $Six2^{GCE}$ or $Cited^{Cre}$ Cre-recombinase-expressing allele developed tumors. The age of onset observed in these two genotypes was similar (Figure 2), and tumor frequency was also similar, despite the increased frequency of recombined cells observed using the $Six2^{GCE}$ allele (Table 1). In contrast, $Wt1$ ablation and biallelic expression of $Igf2$ ($Wt1^{-/fl}$; $H19^{+/-m}$ genotype) resulted in tumors only when nephron progenitors were targeted using the $Cited^{Cre}$ allele (9/18 mice) but not the $Six2^{GCE}$ allele (0/28 mice). When $Cited^{Cre}$ was used to target nephron progenitors, tumors arising following $Wt1$ ablation in the context of $Igf2$ biallelic expression ($C\text{-}Wt1\text{-}Igf2$ mice) developed at a significantly later age ($P = .0058$) than when $Wt1$ was ablated in the context of β-catenin stabilization ($C\text{-}Wt1\text{-}β\text{-}cat^{S}$ mice).

No tumors were observed in animals in which $Wt1$ ablation in the context of either β-catenin stabilization or $Igf2$ biallelic expression was targeted to stromal progenitors ($F\text{-}Wt1\text{-}β\text{-}cat^{S}$ and $F\text{-}Wt1\text{-}Igf2$ cohorts) (Figure 2A, Table 2).

β-Catenin Stabilization Is Sufficient for Tumor Development in Nephron-Progenitor Targeted Cells

Genotyping of tumors confirmed that, as expected, all tumors from $Six2^{GCE}$; $Wt1^{-/fl}$; $Ctnnb1^{+/ex3(fl)}$ animals and $Cited1^{Cre}$; $Wt1^{-/fl}$; $Ctnnb1^{+/ex3(fl)}$ animals carried the recombined $Ctnnb1^{ex3(fl)}$ ($Ctnnb1\text{-}$) allele. Unexpectedly, many tumors (11/14) retained the unrecombined $Wt1^{fl}$ allele (Figure 2B), indicating that $Wt1$ ablation was not required for transformation of the nephron progenitors. $Six2^{GCE}$; $Wt1^{-/fl}$; $Ctnnb1^{+/ex3(fl)}$ mice, $Six2^{GCE}$; $Wt1^{+/fl}$; $Ctnnb1^{+/ex3(fl)}$ mice, $Cited1^{Cre}$; $Wt1^{-/fl}$; $Ctnnb1^{+/ex3(fl)}$ mice, and $Cited1^{Cre}$; $Wt1^{+/fl}$; $Ctnnb1^{+/ex3(fl)}$ mice developed tumors at a similar rate and at similar ages regardless of differential gene dosages of $Wt1$ (Figure 2A). To confirm that β-catenin stabilization alone was sufficient for tumorigenesis, we generated a small cohort of $Six2^{GCE}$; $Ctnnb1^{+/ex3(fl)}$ mice. By 35 weeks of age, 2 of 5 animals developed tumors, similar to the observations in the $Six2^{GCE}$; $Wt1^{-/fl}$; $Ctnnb1^{+/ex3(fl)}$ and $Six2^{GCE}$; $Wt^{+/fl}$; $Ctnnb1^{+/ex3(fl)}$ mice (data not shown).

Of note, $Wt1$ ablation was observed in all tumors from the $Cited1^{Cre}$; $Wt1^{-/fl}$; $H19^{+/-m}$ mice (Figure 2C), and none of the six $Cited1^{Cre}$; $Wt1^{+/fl}$; $H19^{+/-m}$ littermate control mice developed tumors.

Tumor Morphology and Histology

Tumors from the $S\text{-}Wt1\text{-}β\text{-}cat^{S}$ and $C\text{-}Wt1\text{-}β\text{-}cat^{S}$ cohorts were often associated with benign blood-filled cysts, although this occurred less frequently in $C\text{-}Wt1\text{-}β\text{-}cat^{S}$ cohorts. Such cysts were not observed in tumor-bearing $C\text{-}Wt1\text{-}Igf2$ mice. In all three genotypic cohorts,
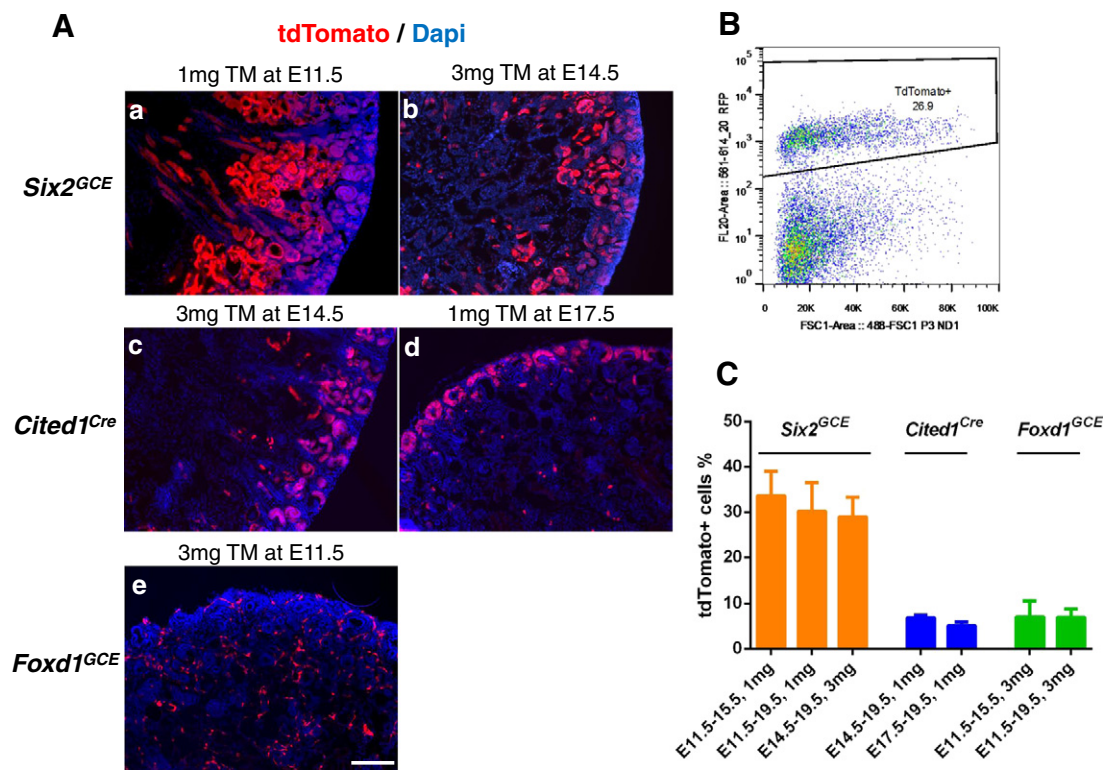
Figure 1. Efficiency of Cre recombination in progenitor-specific Cre lines using $R26^{tdTomato}$ reporter mice. (A) Kidney sections from $Six2^{GCE/+}$; $R26^{tdTomato/+}$ (a and b), $Cited1^{Cre}$; $R26^{tdTomato/+}$ (c and d), and $FoxD1^{GCE/+}$; $R26^{tdTomato/+}$ (e) were treated with TM at indicated time points and analyzed for tdTomato reporter expression at E19.5. DAPI was used to counterstain nuclei. Scale bar: $200\,\mu$m. (B) Representative dot-plot of tdTomato$^+$ cells from single cell suspension of $Cited1^{Cre}$; $R26^{tdTomato/+}$ kidney at E19.5 after 3 mg/40 g BW TM treatment at E14.5. (C) FACS analysis showing percentage of targeted tdTomato$^+$ cells from $Six2^{GCE}$, $Cited1^{Cre}$, and $Foxd1^{GCE}$, respectively. Bar labels indicate the embryonic age at the time of TM injection, the embryonic age at time of kidney collection, and the dose of TM used.

tumors presented as distinct outgrowths from the periphery of the kidney (Figure 3A).

Tumors from the S-$Wt1$-β-cat^S and C-$Wt1$-β-cat^S cohorts displayed an epithelial histology, composed mainly of primitive epithelial cells which formed rosettes (Figure 3B, a and b) and more differentiated epithelial cells which formed tubular structures (Figure 3B, e and f). Stromal elements were observed in areas of some tumors but were generally a very minor feature of the tumors. Blastemal elements were even less frequently observed compared with C-$Wt1$-$Igf2$ tumors. A similar tumor histology was observed irrespective of whether $Wt1$ was ablated.

Targeting Nephron Progenitors with Different Mutations Results in Histologically Different Wilms Tumors

In contrast to the tumors from S-$Wt1$-β-cat^S and C-$Wt1$-β-cat^S cohorts, tumors from the C-$Wt1$-$Igf2$ cohort displayed a triphasic

histology comprised of undifferentiated blastemal, and differentiating epithelial and stromal cells, similar to that observed in the original WT mouse model in which somatic, mosaic $Wt1$ ablation in the context of $Igf2$ biallelic expression was effected using a TM-inducible Cre that is expressed ubiquitously (Figure 3B, c and d) [10].

Expression of β-Catenin and Wnt-β-Catenin Pathway Targets in Tumors

To confirm the stabilization of β-catenin in tumors carrying the $Ctnnb1^{ex3\Delta}$ allele and to assess the impact of this stabilization on the expression of canonical Wnt/β-catenin target genes, we performed IHC for β-catenin and quantified the expression of downstream targets in tumors. As shown in representative tumors in Figure 4A, robust nuclear β-catenin staining was present in tumors from both

Table 1. Efficiency of Progenitor-Specific Cre-Mediated Recombination by FACS Analysis of tdTomato$^+$ Cells with Indicated TM Injection Conditions

Cre	Time point of TM injection	TM dosage	FACS	tdTomato$^+$ cells %
$Six2^{GCE}$	E11.5	1 mg	E15.5	33.7
			E19.5	30.2
	E14.5	3 mg	E19.5	30.0
$Cited1^{Cre}$	E14.5	1 mg	E19.5	6.8
	E17.5	1 mg	E19.5	5.1
$Foxd1^{GCE}$	E11.5	3 mg	E15.5	7.1
			E19.5	7.0

Table 2. Summary of Mouse Mutant Cohorts and TM Injection Conditions

| Designation	Genotype	Tamoxifen (mg/40 g BW)	Tumor mice/ mutant mice
S-Wt1-Igf2	Six2^{GCE}, Wt1$^{-/fl}$, H19$^{+/-m}$	1 at E11.5	0/21
		2 at E14.5	0/7
S-Wt1-β-cat^S	Six2^{GCE}, Wt1$^{-/fl}$, β-cat$^{e3+/fl}$	3 at E14.5	8/11 (73%)
	Six2^{GCE}, Wt1$^{+/fl}$, β-cat$^{e3+/fl}$	3 at E14.5	6/12 (50%)
S-β-cat^S	Six2^{GCE}, β-cat$^{e3+/fl}$	3 at E14.5	2/5 (40%)
C-Wt1-Igf2	Cited1^{Cre}, Wt1$^{-/fl}$, H19$^{+/-m}$	1 at E14.5	9/18 (50%)
C-Wt1-β-cat^S	Cited1^{Cre}, Wt1$^{-/fl}$, β-cat$^{e3+/fl}$	0.5 at E17.5	9/20 (45%)
	Cited1^{Cre}, Wt1$^{+/fl}$, β-cat$^{e3+/fl}$	0.5 at E17.5	3/7 (43%)
F-Wt1-Igf2	Foxd1^{GCE}, Wt1$^{-/fl}$, H19$^{+/-m}$	3 at E11.5	0/9
F-Wt1-β-cat^S	Foxd1^{GCE}, Wt1$^{-/fl}$, β-cat$^{e3+/fl}$	3 at E11.5	0/17
	Foxd1^{GCE}, Wt1$^{+/fl}$, β-cat$^{e3+/fl}$	3 at E11.5	0/11
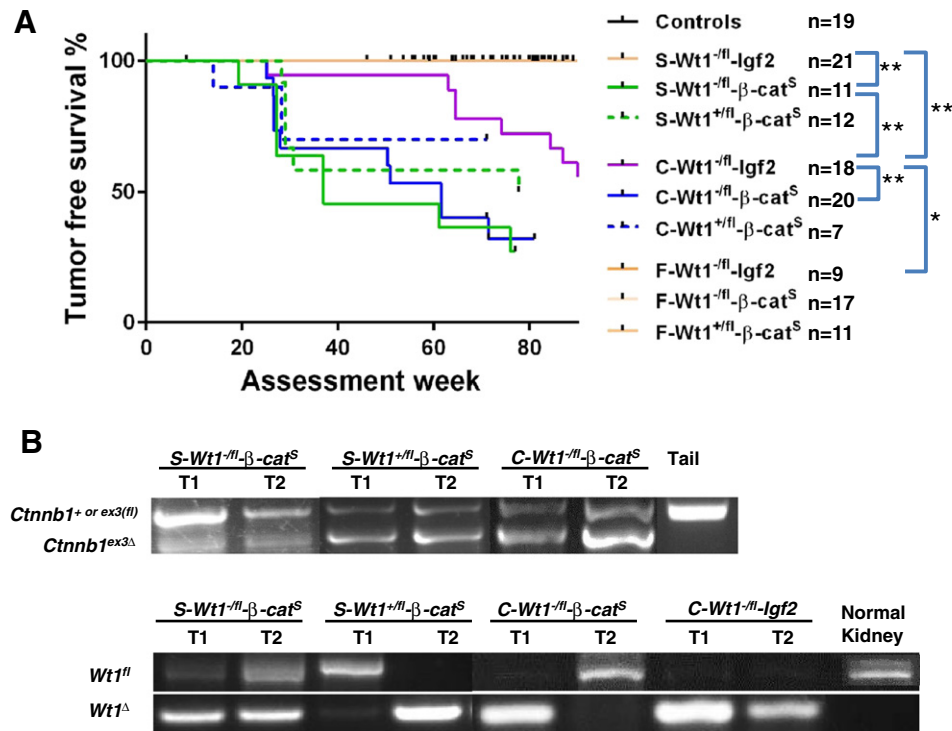
Figure 2. Development of WT from nephron progenitors. (A) Kaplan-Meier tumor-free survival analysis showing incidence of WT in $Six2^{GCE}$, $Cited1^{Cre}$, and $Foxd1^{GCE}$ mutant mice with Wt1 ablation/haploinsufficiency and β-catenin stabilization ($S/C/F$-$Wt1^{-/fl}$-β-cat^S and $S/C/F$-$Wt1^{+/fl}$-β-cat^S) and Wt1 ablation and Igf2 upregulation ($S/C/F$-$Wt1^{-/fl}$-$Igf2$) in comparison to control mice. (B) PCR analysis of DNA from mutant mice showing $Ctnnb1$ wild-type or exon3 floxed allele and exon3 deleted allele ($Ctnnb1^{+}$ or $Ctnnb1^{ex3(fl)}$ and $Ctnnb1^{ex3\Delta}$) and $Wt1$ floxed or null alleles ($Wt1^{fl}$ or $Wt1^{\Delta}$).
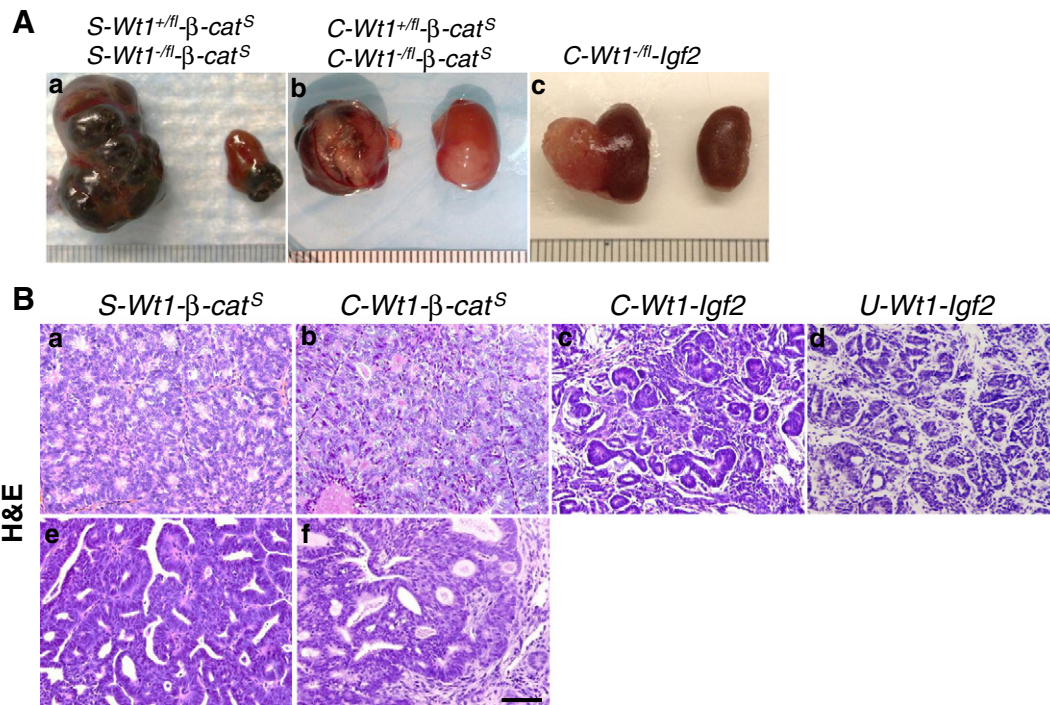

Figure 3. Histological analysis of WTs from $Six2^{GCE}$ and $Cited1^{Cre}$ mice. (A) Gross appearance of tumors from $Six2^{GCE}$ mice (a) and $Cited1^{Cre}$ mice (b and c) of the indicated genotypes. (B) H&E staining of kidney tumor sections of S-$Wt1$-β-cat^S, C-$Wt1$-β-cat^S, and C-$Wt1$-$Igf2$ mice. Scale bar: 100 μm.

S-Wt1-β-cat^S and C-Wt1-β-cat^S cohorts. The presence or absence of Wt1 ablation did not affect this robust staining (data not shown). However, β-catenin in the C-Wt1-Igf2 tumors was primarily cytoplasmic (Figure 4A).

Tumors in which β-catenin was stabilized generally displayed increased expression of Axin2, Wif1, and Dkk2, genes previously reported to be upregulated upon Wnt/β-catenin activation, although there was considerable tumor variability in the expression of Axin2 and Dkk2. Despite this variability, there were significant differences in Axin2 expression between Cited1^{Cre}-targeted tumors with β-catenin stabilization versus Cited1^{Cre}-targeted tumors with Wt1 ablation and Igf2 biallelic expression. Upregulation of Wif1 was less variable and was dramatically increased in β-catenin stabilized tumors. Within the same Cited1^{Cre}-targeted progenitor population, increased Wif1 expression was observed in the C-Wt1-β-cat^S tumors but not the C-Wt1-Igf2 tumors, consistent with Wif1 being a target of the Wnt/β-catenin pathway. Unexpectedly, contrasting data were obtained for CyclinD1 and C-myc, two other Wnt/β-catenin targets whose expression was significantly higher in tumors not carrying the stabilizing Ctnnb1 mutation (Figure 4B).

Tumors from S-Wt1-β-cat^S and C-Wt1-β-cat^S Mice Have Different Expression Patterns of Differentiation Markers than Tumors from C-Wt1-Igf2 Mice

Differential expression of genes variably expressed in different renal lineages and at different stages of differentiation was noted between subsets of human Wilms tumors, and these data were used to construct a model of the cellular ontogeny of Wilms tumors [9]. Having targeted

different sets of mutations to different cellular compartments of the developing kidney, we were in a position to test whether resulting tumors displayed differential expression of these developmentally regulated genes.

Tumors arising following the targeting β-catenin stabilization to committed epithelial progenitors—by either Six2^{GCE} or Cited1^{Cre}—displayed low expression of genes primarily expressed in the intermediate renal mesenchyme and/or later metanephric mesenchyme (Eya1, Osr1, Pax2, and Hoxa11) (Figure 5). However, targeting Wt1 ablation in the context of Igf2 biallelic expression to nephron progenitors using the same Cited1^{Cre} transgene resulted in tumors that robustly expressed these early stage genes. This expression of early mesenchymal genes was similar to that observed in tumors when the same mutations were introduced via the ubiquitously expressed Cre-ER^{TM} allele in the original WT mouse model (Figure 5) [10,19]. Robust expression of Wnt4 and Jag1, markers of induced mesenchyme, and CyclinD1, whose expression is transiently upregulated following induction, was observed only in tumors with Wt1 ablation and Igf2 biallelic expression. Expression of muscle differentiation genes was often variable between tumors within a cohort and also between cohorts (Supplementary Figure 1). Whereas a statistically significant increase in expression was observed for some genes, e.g., Pax3 in Cited1-β-cat^S and Six1-Wt1-β-cat^S tumors and Ttn in Cited1-Wt1-Igf2 tumors, this was not consistent across the three muscle differentiation genes we assessed.

Assessment of protein expression by IHC staining confirmed that S-Wt1-β-cat^S and C-Wt1-β-cat^S tumors did not express PAX2 or
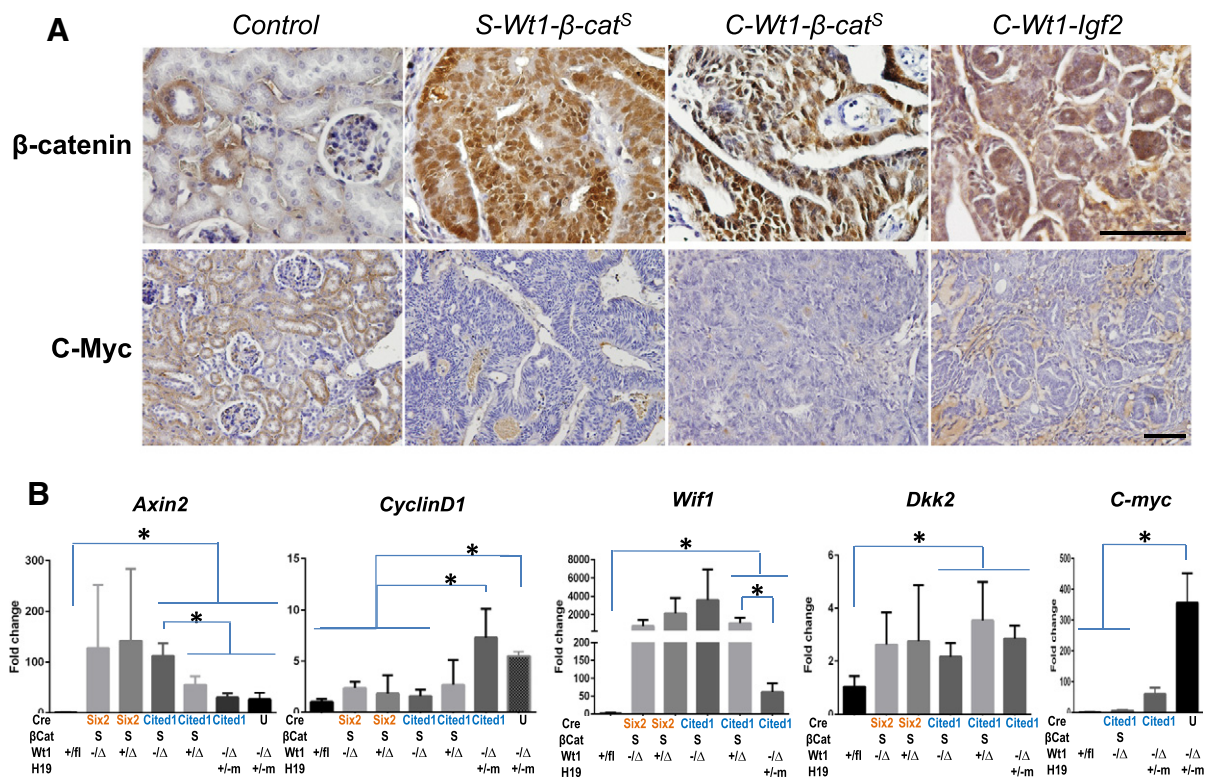
Figure 4. Activity of Wnt/β-catenin signaling in mouse WTs. (A) IHC staining of β-catenin and C-myc for sections from control kidneys and tumors from S-Wt1-β-cat^S, C-Wt1-β-cat^S, and C-Wt1-Igf2 mutants. Scale bar: 100 μm. (B) qPCR analysis of Wnt/β-catenin canonical effectors Axin2, CyclinD1, and C-myc and signaling inhibitors Wif1 and Dkk2 in littermate kidneys and tumors from S-Wt1-β-cat^S, C-Wt1-β-cat^S, and C-Wt1-Igf2 mutants. The x-axis labels indicate wild-type (Wt1$^{+/fl}$) in littermate kidneys and the presence of progenitor-specific Cre alleles (Six2^{GCE} or Cited1^{Cre}) or Ubiquitous-Cre (U) and the presence of genetic alterations of β-cat^S, Wt1 ablation (Wt1$^{-/}$) or Igf2 upregulation (H19$^{+/-m}$) in mouse tumors.
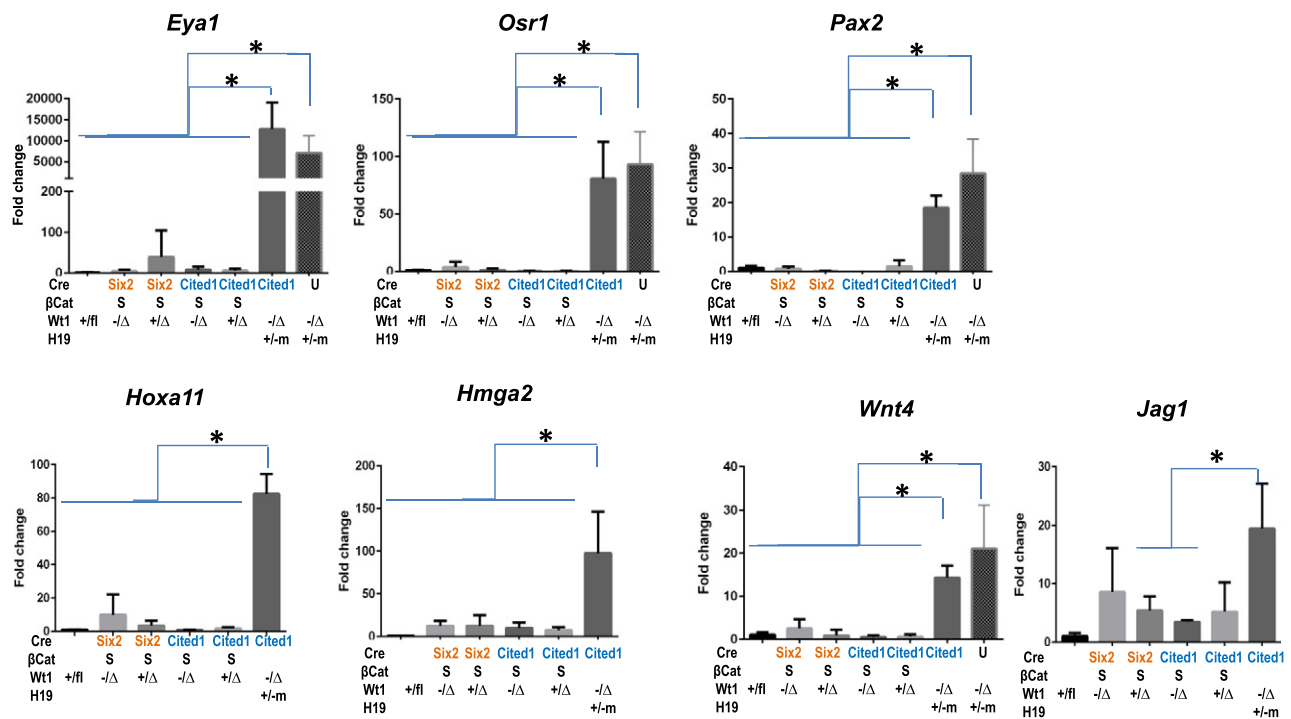
Figure 5. Expression of differentiation markers in WTs of $Six2^{GCE}$ and $Cited1^{Cre}$ mice. qPCR analysis of early metanephric mesenchyme markers ($Eya1$, $Osr1$, $Pax2$, $Hoxa11$, and $Hmga2$) and renal vesicle markers ($Wnt4$ and $Jag1$) in littermate kidneys and tumors from S-$Wt1$-β-cat^S, C-$Wt1$-β-cat^S, and C-$Wt1$-$Igf2$ mutants. The x-axis labels indicate wild-type (Wt1 $^{+/fl}$) in littermate kidneys and the presence of progenitor-specific Cre alleles ($Six2^{GCE}$ or $Cited1^{Cre}$) or Ubiquitous-Cre (U) and the presence of genetic alterations of β-cat^S, $Wt1$ ablation ($Wt1$ $^{-/}$) or $Igf2$ upregulation ($H19^{+/-m}$) in mouse tumors.

CYCLIND1, whereas C-$Wt1$-$Igf2$ tumors robustly expressed PAX2. All three tumor types expressed CITED1, a marker of nephron progenitors and, in epithelial elements, expressed E-cadherin, a marker of terminally differentiated epithelium.

In summary, both gene and protein expression data revealed that C-$Wt1$-$Igf2$ tumors expressed markers of early mesenchyme and also postinduction genes, whereas S-$Wt1$-β-cat^S and C-$Wt1$-β-cat^S tumors expressed markers of committed nephron progenitors and epithelial differentiation.

Discussion

Classically, three cell types—blastemal, stromal, and epithelial—are observed in Wilms tumors, and such triphasic tumors have been thought to arise from early undifferentiated metanephric mesenchyme. However, the observation of tumors comprised predominantly of stromal or epithelial elements has led to the suggestion that these tumors arise from fetal kidney cells committed to a stromal or epithelial lineage. The main goals of the current study were to determine if tumors could arise from such committed progenitors and, if they did, whether the resultant tumors displayed a characteristic histology and whether the type of genetic alterations introduced into renal progenitors affected their tumorigenicity and/or the histology of the resulting tumors.

Using a Cre-LoxP approach, we earlier demonstrated that random somatic and mosaic $Wt1$ ablation in the context of $Igf2$ biallelic expression, a combination of alterations observed in human Wilms tumors, resulted in mouse tumors with a classic triphasic histology [10]. We have now introduced that same set of mutations and also the combination of $Wt1$ ablation and β-catenin stabilization, another combination that is also observed in human WTs [11], into specific

cellular compartments of the developing kidney using TM-inducible Cre-expressing alleles that target kidney stromal progenitors or nephron progenitors.

Confirmation of Appropriate Targeting of Kidney Progenitors

Our lineage tracing experiments confirmed the expected progenitor-specific expression of each of the Cre alleles employed in the study: kidney stroma was derived from $FoxD1^{GCE}$-tdTomato–tagged cells, whereas $Six2^{GCE}$-tagged and $Cited1^{Cre}$-tagged cells were present in the cap mesenchyme population at early time points following Cre induction and at later time point in the comma-shaped and S-shaped bodies of developing nephrons and also the tubules and glomeruli of mature nephrons. Interestingly, the tdTomato$^+$ cells present 5 days following targeting by $Six2^{GCE}$ existed in more mature structures than those present 5 days following targeting by $Cited1^{Cre}$ at the same time point. $Six2^{GCE}$-tdTomato$^+$ cells also represented a larger percentage of the total kidney cell population than $Cited1$-^{Cre}-tdTomato$^+$ cells. Both SIX2 and CITED1 have been identified as markers for committed nephron progenitors, which are ultimately induced to undergo a mesenchyme-epithelial transition in response to WNT9b from the ureteric bud [4,5]. However, recent work suggests a more nuanced compartmentalization in which CITED1$^+$ SIX2$^+$ cells, which are nonresponsive to WNT9b induction, lose expression of CITED1, resulting in SIX2$^+$-only cells that do respond to WNT9b-induced epithelialization [8]. Thus, CITED1$^+$ SIX2$^+$ cells are proposed to represent the self-renewing nephron progenitor compartment, whereas SIX2$^+$ cells represent cells that can then respond to WNT9b and β-catenin.

Our observation of more differentiated $tdTomato^+$ cells following targeting by $Six2^{GCE}$ is consistent with this model. Unlike the $Cited1$-

targeted population, the $Six2$-targeted population would include cells on the cusp of epithelial differentiation, resulting in $Six2^{GCE}$-tdTomato$^+$ cells being observed at later stages of nephron development. This model could also account for the greater proportion of $Six2^{GCE}$-tdTomato$^+$ cells than $Cited1^{Cre}$-tdTomato$^+$ cells 5 days following TM-induced $tdTomato$ expression.

Tumors Develop Following Mutational Targeting of Nephron Progenitors

Tumors were observed in both the S-$Wt1$-β-cat^S and C-$Wt1$-β-cat^S cohorts, demonstrating that Wilms tumors can arise from committed nephron progenitors. Interestingly, a similar frequency of tumor development and age of onset was observed in mice following targeting of $Wt1$ ablation and β-catenin stabilization with $Cited1^{Cre}$ or $Six2^{GCE}$, despite the $tdTomato$-lineage tracing data that indicated a five-fold increase in the percentage of cells following $Six2^{GCE}$- versus $Cited1^{Cre}$-induced labeling. This observation could be due to the rapid differentiation of $Six2^{GCE}$-tdTomato$^+$ cells to a more differentiated cell type that was refractory to transformation by the introduced mutations. A previous study reported development of mouse primitive epithelial tumors with features of Wilms tumors by using $Cited1^{Cre}$ to activate β-catenin with or without K-ras activation postnatally [20]. In this study, a proximal tubule specific γGT-Cre was also applied to activate β-catenin, and K-ras and mutant mice developed metastases to the lungs in addition to the primitive epithelial tumors [20]. These tumors appeared histologically very similar to our S-$Wt1$-β-cat^S and C-$Wt1$-β-cat^S epithelial Wilms tumors. In our study, Six2^{GCE} or Cited1^{Cre} was activated at an early stage of kidney development, and nephron progenitors were targeted, which was different from the approach of targeting cells postnatally in their models. Moreover, in S-$Wt1$-β-cat^S and C-$Wt1$-β-cat^S mutants, a strong association of cystic kidney phenotype was observed with tumor development. Combined, these results suggest that, with β-catenin activation, both nephron progenitors and proximal tubules can give rise to renal epithelial tumors in mice.

Another striking and statistically significant difference between $Six2^{GCE}$- versus $Cited1^{Cre}$-targeted cohorts was the tumorigenic effect of the combination of $Wt1$ ablation and $Igf2$ biallelic expression. No tumors arose in S-$Wt1$-$Igf2$ animals (in which both the CITED1$^+$ SIX2$^+$ and the SIX2$^+$-only progenitor populations were targeted), whereas 50% (9/18) of C-$Wt1$-$Igf2$ animals (in which only the CITED1$^+$ SIX2$^+$ population is expected to be targeted) developed tumors (Figure 2A, Table 2). These differences between the $Six2^{CGE}$ and $Cited1^{Cre}$ cohorts may be due to differences in the cells targeted by these two Cre alleles. In the metanephric mesenchyme surrounding the ureteric bud, two compartments, one CITED1$^+$ SIX2$^+$ and one SIX2$^+$ only, have been delineated [7,8]. Whereas the robust expression of the Cre alleles in the metanephric mesenchyme surrounding the ureteric bud has been demonstrated by immunofluorescence analysis [5], less robust expression of these alleles elsewhere in the developing mesenchyme is possible and perhaps to be expected given that endogenous $Six2$ and $Cited1$ expression is observed at low levels at earlier stages of kidney development [12,21,22]. Of note, in contrast to the frequent co-occurrence of $Ctnnb1$ and $WT1$ mutations in human Wilms tumors [11], Sanger sequencing revealed that C-$Wt1$-$Igf2$ mouse tumors did not spontaneously acquire $Ctnnb1$ mutations (Huff, unpublished).

Another possible explanation for the difference in the tumorigenic effect of $Wt1$ ablation and $Igf2$ biallelic expression in the $Six2^{CGE}$

versus the $Cited1^{Cre}$ cohort could be related to the experimental approaches used for this study which result in additional differences in $Six2^{GCE}$- and $Cited1^{Cre}$-targeted cells. Animals carrying the $Six2^{GCE}$ allele in which the Cre-GFP cassette is knocked into the $Six2$ locus are effectively $Six2^{+/-}$. $Six2$ encodes a transcription factor that plays an important role in nephron progenitor self-renewal [23,5,24]. Whereas $Six2^{+/-}$ mice have no discernable kidney phenotype [25], suggesting that nephron progenitor self-renewal is unaffected by $Six2$ haploinsufficiency, such haploinsufficiency could plausibly impact the ability of $Ctnnb1$-mutant cells to become tumors. SIX2 and β-catenin are reported to act in both an opposing and a cooperative manner to regulate different subsets of genes during epithelialization of induced nephron progenitors [24]. If $Six2$ haploinsufficiency is a factor in the differential tumor development in our experimental cohorts, the data would suggest that, in the context of β-catenin stabilization, $Six2$ haploinsufficiency helps to promote tumorigenesis of nephron progenitors or that $Six2$ haploinsufficiency is incompatible with tumor development in the context of $Wt1$ ablation and biallelic $Igf2$ expression. Heterozygous SIX2 missense mutations are observed in human Wilms tumors and are often coincident with mutations in miRNA processing genes [26,27]. Neither $WT1$ nor $CTNNB1$ mutations were observed in SIX2-mutant tumors. These data are consistent with the model that, in our mice, $Six2$ haploinsufficiency was not a factor in the differential tumor development we observed between the $Six2$-Cre and $Cited1$-Cre cohorts upon the introduction of $Wt1$ and $Ctnnb1$ mutations, although further studies will be required to test this experimentally. Of note, in human tumors, $IGF2$ loss of heterozygosity or loss of imprinting (which results in biallelic expression) is very common and is observed irrespective of SIX2 mutation [26,27].

Previously, we used a ubiquitously expressing Cre transgene to mosaically ablate $Wt1$ in the genetic background of $Igf2$ upregulation (U-$Wt1$-$Igf2$) [26]. These mice had an earlier onset (10 weeks) and a higher frequency of tumor development (80%) than the C-$Wt1$-$Igf2$ tumors in the current study (onset at 25th week and an overall tumor frequency of 50%). Although these two models carry the same genetic mutations, the differences in tumor onset and penetration may be due to differences in the differentiation status of the cells when the mutations are introduced. Many human tumors are thought to arise from intermediate mesoderm which may be the cell of origin for the U-$Wt1$-$Igf2$ tumors, as opposed to the more differentiated cells that were targeted by use of the $Cited1$-Cre transgene.

Transformation of Nephron Progenitors by β-Catenin Stabilization Does Not Require Wt1 Ablation

$WT1$ ablation and $CTNNB1$ mutation that result in β-catenin stabilization are highly concordant in human Wilms tumors [11,9]. All $CTNNB1$ mutations reported to date are somatic and those that affect residues encoded in exon 3 that are critical for β-catenin stability almost invariably occur in the presence of $Wt1$ ablation [11,9,28]. Thus, our observation when we genotyped mouse tumors from $Six2^{GCE}$; $Wt1^{-/fl}$; $Ctnnb1^{+/ex3(fl)}$ and $Cited^{Cre}$; $Wt1^{-/fl}$; $Ctnnb1^{+/ex3(fl)}$ mice that only one of six tumors displayed complete $Wt1$ ablation was highly unexpected. Because this was observed in both the S-$Wt1$-β-cat^S and C-$Wt1$-β-cat^S cohort tumors, $Six2$ haploinsufficiency is likely not a factor in this unexpected finding. In addition, the presence or absence of $Wt1$ ablation did not result in a statistically significant difference in the frequency or age at which tumors developed. Cohorts with a $Wt1^{-/fl}$ genotype developed

tumors similar to mice with a $Wt1^{+/fl}$ genotype, as did mice with a $Wt1^{+/+}$ genotype (Figure 2). Although analysis of larger cohorts might, in the future, identify subtle differences in tumor susceptibility between these different genotypes, the current data demonstrate that $Wt1$ ablation in addition to β-catenin stabilization is not required for tumorigenesis of nephron progenitors.

The observation that $Ctnnb1$ mutation targeted to nephron progenitors resulted in tumors in the absence of $Wt1$ mutations is in interesting contrast with human tumors in which $CTNNB1$ mutations are frequently associated with $WT1$ mutations [11]. In addition, a subset of human tumors (subset 1) proposed to arise from postinduction nephron progenitors carries neither $Ctnnb1$ nor $Wt1$ mutations [9], although, like the $Ctnnb1$-mutant mouse tumors arising from targeted nephron progenitors, they exhibit a differentiated epithelial histology.

Whether $Ctnnb1$ mutation is sufficient for cell transformation in uncommitted metanephric mesenchyme is not known. Somatic deletion of exon 3 of $Ctnnb1$ using the ubiquitously expressing inducible Cre allele resulted in embryonic lethality even when Cre activity was induced in <5% of cells (Huff, unpublished data). This observation is consistent with the importance of the Wnt/β-catenin pathway and its precise regulation in many developmental processes. Thus, the assessment of the ability of β-catenin stabilization alone to transform uncommitted cells of the embryonic kidney awaits the use of a Cre allele that specifically targets these cells.

Histologic and Gene Expression Differences between Tumors

Tumors from C-$Wt1$-$β$-cat^S and S-$Wt1$-$β$-cat^S cohorts were primarily composed of epithelial cells with few stromal and negligible blastemal components. This is consistent with observations that Wnt pathway activation stimulates epithelialization of induced SIX2⁺-only nephron progenitors [29,8]. The epithelial histology of these mouse tumors when a committed nephron progenitor is targeted is similar to that observed in human subset 1 tumors which are thought to arise late in kidney development [9]. Interestingly, $CTNNB1$ mutations are not present in S1 tumors [9]. These data suggest that, for the differentiated epithelial-predominant tumors, cell ontogeny plays a bigger role in determining tumor histology than does the genetic alteration present.

In contrast to the histology of tumors from C-$Wt1$-$β$-cat^S and S-$Wt1$-$β$-cat^S cohorts, stromal and blastemal cells were more frequent in tumors from C-$Wt1$-$Igf2$ cohorts, although not to the extent observed when a ubiquitously expressed Cre allele was employed to ablate $Wt1$ in the context of $Igf2$ biallelic expression (Figure 1). In general, differences in gene expression were also observed between genotypes rather than between the Cre alleles used to target cells. With few exceptions, no difference in gene expression was observed between tumors from S-$Wt1$-$β$-cat^S and tumors from C-$Wt1$-$β$-cat^S mice. In contrast, tumors from S-$Wt1$-$β$-cat^S and C-$Wt1$-$β$-cat^S mice were significantly different from tumors from C-$Wt1$-$Igf2$ mice, and the latter tumors were very similar to U-$Wt1$-$Igf2$ tumors with respect to the expression of genes expressed during kidney development that are targets of Wnt/β-catenin signaling.

Like human subset 2 and 3 tumors in which $WT1$ and $CTNNB1$ mutations are frequently observed (along with $IGF2$ LOH/LOI), genes normally expressed in intermediate mesoderm and early metanephric mesenchyme were highly expressed in both C-$Wt1$-$Igf2$ and U-$Wt1$-$Igf2$ tumors relative to normal kidney and to tumors from the S-$Wt1$-$β$-cat^S and C-$Wt1$-$β$-cat^S cohorts (Figure 5). This is of particular interest because the expression of intermediate mesoderm genes is more concordant with tumor genotype than it is with the Cre transgene used for introducing gene alterations. Like human S2 and S3 tumors, it has been suggested that the U-$Wt1$-$Igf2$ tumors arise from intermediate mesoderm or early metanephric mesenchyme, in large part due to the fetal age (~E12) at which the alterations were induced. The observation of tumors with a similar histology and a similar gene expression profile following the introduction of those same alterations at a much later stage of kidney development (~E18) is unexpected. Of note, C-$Wt1$-$β$-cat^S tumors did not display a predominant histology of blastemal cells that are most reminiscent of intermediate mesenchyme. These data suggest that $Wt1$ ablation and $Igf2$ biallelic expression, but not $Ctnnb1$ mutation, in the $Cited^{Cre}$-targeted committed nephron progenitors result in the reexpression of these early genes and/or results in partial dedifferentiation of these cells which secondarily results in expression of these genes. The fact that the C-$Wt1$-$Igf2$ and U-$Wt1$-$Igf2$ tumors (but not tumors from S-$Wt1$-$β$-cat^S and C-$Wt1$-$β$-cat^S mice) also displayed increased expression of two genes, $Wnt4$ and $Jag1$, that characterize nephron progenitors induced to epithelialize and that are subsequently downregulated is consistent with the presence of epithelial elements in the tumors, in additional to blastemal and stromal elements.

S2 and S3 tumors also showed expression of genes associated with muscle differentiation (e.g., $MYH3$, TTN, $ACTA1$) as compared with other tumor subsets, although heterologous muscle elements were often not observed histologically. Such elements were not observed in the mouse tumors, although we did observe a statistically significant, but variable, upregulation of $Pax3$, Ttn, and $Acta1$ in mouse tumors compared with normal kidney (Supplementary Figure 1).

Lack of Tumor Development Following Mutational Targeting of Stromal Progenitors

In contrast to the tumor development observed when nephron progenitors were targeted, no tumors were observed when mutations were targeted to renal stromal progenitors using the $Foxd1^{GCE}$ Cre allele (Table 2). Although it is possible that these progenitors have a low-level capacity to be transformed by either combination of alterations we introduced (or by different alterations that were not tested here), these data demonstrate that there is a statistically significant difference in the tumorigenic potential of these two different progenitor populations. Human tumors that, from gene expression profiling, are thought to arise from a similar population of undifferentiated metanephric mesenchyme display varying histologies, including a mixed triphasic histology and a stromal predominant histology, even in tumors with $WT1$ mutations [9]. Thus, the human data and the mouse data presented here suggest that the presence—and sometimes even the predominance—of stromal elements in tumors is not necessarily due to these tumors arising from a committed stromal progenitor. Rather, a stromal histology may be the result of aberrant intermediate renal mesoderm whose normal constraints on cell fate decisions are loosened, resulting in tumors with varying populations of cell types normally observed upon differentiation—e.g., ductal epithelium and stroma—along with heterologous elements (muscle and cartilage). These data, however, do not preclude the possibility that some tumors do arise from stroma.

Conclusions

In sum, these data suggest that mutation of nephron progenitors, but not stromal progenitors, results in tumor development, at least with

the sets of alterations introduced and the time points at which they were introduced into the progenitors. Using gene expression data from human tumors, a model for Wilms tumor ontogeny was developed such that tumors expressing genes characteristic of intermediate mesoderm or early metanephric mesenchyme were proposed to have arisen from cells at these early stages of kidney development. Although this may be the case in general, our experimental data in mice indicate that, even at a later stage, committed nephron progenitors can give rise to tumors. In the case of *Ctnnb1* mutation, tumors arising from these progenitors are histologically well differentiated and do not express genes characteristic of earlier stages of kidney development. However, tumors with a more triphasic histology and expression of these early kidney genes are observed when *Wt1* ablation and *Igf2* biallelic expression are introduced. These data suggest that this combination of alterations can effect a reprogramming of committed nephron progenitors. This model is supported by the observations that ablation of *Wt1* results in a block in differentiation of the metanephric mesenchyme [10] and that, in the testes, *Wt1* ablation results in the transdifferentiation of Sertoli cells to fetal-like Leydig cells [30].

C-Wt1-Igf2 tumors were similar histologically and with respect to gene expression to tumors rising from the nontargeted introduction of these same alterations into fetal kidney (*U-Wt1-Igf2* tumors). Whether this is due to the ability of these alterations to reprogram committed nephron progenitors to an early metanephric mesenchyme state or because the *U-Wt1-Igf2* tumors arise from committed nephron progenitors is not known. The two sets of tumors do differ with respect to the expression of *C-myc*, suggesting some difference in tumor ontogeny. It will be informative in the future to specifically target early metanephric mesenchyme and determine the tumorigenicity of these cells and the histologic and gene expression characteristics of resulting tumors.

Supplementary data to this article can be found online at http://dx.doi.org/10.1016/j.neo.2015.12.001.

Acknowledgements

References

[1] Mugford JW, Sipila P, McMahon JA, and McMahon AP (2008). Osr1 expression demarcates a multi-potent population of intermediate mesoderm that undergoes progressive restriction to an Osr1-dependent nephron progenitor compartment within the mammalian kidney. *Dev Biol* **324**, 88–98.

[2] Kobayashi A, Mugford JW, Krautzberger AM, Naiman N, Liao J, and McMahon AP (2014). Identification of a multipotent self-renewing stromal progenitor population during mammalian kidney organogenesis. *Stem Cell Reports* **3**, 650–662.

[3] Brunskill EW, Park JS, Chung E, Chen F, Magella B, and Potter SS (2014). Single cell dissection of early kidney development: multilineage priming. *Development* **141**, 3093–3101.

[4] Boyle S, Misfeldt A, Chandler KJ, Deal KK, Southard-Smith EM, Mortlock DP, Baldwin HS, and de Caestecker M (2008). Fate mapping using Cited1-CreERT2 mice demonstrates that the cap mesenchyme contains self-renewing progenitor cells and gives rise exclusively to nephronic epithelia. *Dev Biol* **313**, 234–245.

[5] Kobayashi A, Valerius MT, Mugford JW, Carroll TJ, Self M, Oliver G, and McMahon AP (2008). Six2 defines and regulates a multipotent self-renewing nephron progenitor population throughout mammalian kidney development. *Cell Stem Cell* **3**, 169–181.

[6] Humphreys BD, Lin SL, Kobayashi A, Hudson TE, Nowlin BT, Bonventre JV, Valerius MT, McMahon AP, and Duffield JS (2010). Fate tracing reveals the pericyte and not epithelial origin of myofibroblasts in kidney fibrosis. *Am J Pathol* **176**, 85–97.

[7] Mugford JW, Yu J, Kobayashi A, and McMahon AP (2009). High-resolution gene expression analysis of the developing mouse kidney defines novel cellular compartments within the nephron progenitor population. *Dev Biol* **333**, 312–323.

[8] Brown AC, Muthukrishnan SD, Guay JA, Adams DC, Schafer DA, Fetting JL, and Oxburgh L (2013). Role for compartmentalization in nephron progenitor differentiation. *Proc Natl Acad Sci U S A* **110**, 4640–4645.

[9] Gadd S, Huff V, Huang CC, Ruteshouser EC, Dome JS, Grundy PE, Breslow N, Jennings L, Green DM, and Beckwith JB, et al (2012). Clinically relevant subsets identified by gene expression patterns support a revised ontogenic model of Wilms tumor: a Children's Oncology Group Study. *Neoplasia* **14**, 742–756.

[10] Hu Q, Gao F, Tian W, Ruteshouser EC, Wang Y, Lazar A, Stewart J, Strong LC, Behringer RR, and Huff V (2011). Wt1 ablation and Igf2 upregulation in mice result in Wilms tumors with elevated ERK1/2 phosphorylation. *J Clin Invest* **121**, 174–183.

[11] Maiti S, Alam R, Amos CI, and Huff V (2000). Frequent association of beta-catenin and WT1 mutations in Wilms tumors. *Cancer Res* **60**, 6288–6292.

[12] Boyle S, Shioda T, Perantoni AO, and de Caestecker M (2007). Cited1 and Cited2 are differentially expressed in the developing kidney but are not required for nephrogenesis. *Dev Dyn* **236**, 2321–2330.

[13] Madisen L, Zwingman TA, Sunkin SM, Oh SW, Zariwala HA, Gu H, Ng LL, Palmiter RD, Hawrylycz MJ, and Jones AR, et al (2010). A robust and high-throughput Cre reporting and characterization system for the whole mouse brain. *Nat Neurosci* **13**, 133–140.

[14] Kreidberg JA, Sariola H, Loring JM, Maeda M, Pelletier J, Housman D, and Jaenisch R (1993). WT-1 is required for early kidney development. *Cell* **74**, 679–691.

[15] Gao F, Maiti S, Alam N, Zhang Z, Deng JM, Behringer RR, Lecureuil C, Guillou F, and Huff V (2006). The Wilms tumor gene, Wt1, is required for Sox9 expression and maintenance of tubular architecture in the developing testis. *Proc Natl Acad Sci U S A* **103**, 11987–11992.

[16] Harada N, Tamai Y, Ishikawa T, Sauer B, Takaku K, Oshima M, and Taketo MM (1999). Intestinal polyposis in mice with a dominant stable mutation of the beta-catenin gene. *EMBO J* **18**, 5931–5942.

[17] Leighton PA, Ingram RS, Eggenschwiler J, Efstratiadis A, and Tilghman SM (1995). Disruption of imprinting caused by deletion of the H19 gene region in mice. *Nature* **375**, 34–39.

[18] Mokkapati S, Niopek K, Huang L, Cunniff KJ, Ruteshouser EC, deCaestecker M, Finegold MJ, and Huff V (2014). beta-catenin activation in a novel liver progenitor cell type is sufficient to cause hepatocellular carcinoma and hepatoblastoma. *Cancer Res* **74**, 4515–4525.

[19] Hayashi S and McMahon AP (2002). Efficient recombination in diverse tissues by a tamoxifen-inducible form of Cre: a tool for temporally regulated gene activation/inactivation in the mouse. *Dev Biol* **244**, 305–318.

[20] Clark PE, Polosukhina D, Love H, Correa H, Coffin C, Perlman EJ, de Caestecker M, Moses HL, and Zent R (2011). beta-Catenin and K-RAS synergize to form primitive renal epithelial tumors with features of epithelial Wilms' tumors. *Am J Pathol* **179**, 3045–3055.

[21] Oliver G, Wehr R, Jenkins NA, Copeland NG, Cheyette BN, Hartenstein V, Zipursky SL, and Gruss P (1995). Homeobox genes and connective tissue patterning. *Development* **121**, 693–705.

[22] Dunwoodie SL, Rodriguez TA, and Beddington RS (1998). Msg1 and Mrg1, founding members of a gene family, show distinct patterns of gene expression during mouse embryogenesis. *Mech Dev* **72**, 27–40.

[23] Bouchard M, Souabni A, Mandler M, Neubuser A, and Busslinger M (2002). Nephric lineage specification by Pax2 and Pax8. *Genes Dev* **16**, 2958–2970.

[24] Park JS, Ma W, O'Brien LL, Chung E, Guo JJ, Cheng JG, Valerius MT, McMahon JA, Wong WH, and McMahon AP (2012). Six2 and Wnt regulate self-renewal and commitment of nephron progenitors through shared gene regulatory networks. *Dev Cell* **23**, 637–651.

[25] Self M, Lagutin OV, Bowling B, Hendrix J, Cai Y, Dressler GR, and Oliver G (2006). Six2 is required for suppression of nephrogenesis and progenitor renewal in the developing kidney. *EMBO J* **25**, 5214–5228.

[26] Walz AL, Ooms A, Gadd S, Gerhard DS, Smith MA, Guidry Auvil JM, Meerzaman D, Chen QR, Hsu CH, and Yan C, et al (2015). Recurrent DGCR8, DROSHA, and SIX homeodomain mutations in favorable histology Wilms tumors. *Cancer Cell* **27**, 286–297.

[27] Wegert J, Ishaque N, Vardapour R, Georg C, Gu Z, Bieg M, Ziegler B, Bausenwein S, Nourkami N, and Ludwig N, et al (2015). Mutations in the SIX1/2 pathway and the DROSHA/DGCR8 miRNA microprocessor complex underlie high-risk blastemal type Wilms tumors. *Cancer Cell* **27**, 298–311.

[28] Fukuzawa R, Heathcott RW, More HE, and Reeve AE (2007). Sequential WT1 and CTNNB1 mutations and alterations of beta-catenin localisation in intralobar nephrogenic rests and associated Wilms tumours: two case studies. *J Clin Pathol* **60**, 1013–1016.

[29] Kuure S, Popsueva A, Jakobson M, Sainio K, and Sariola H (2007). Glycogen synthase kinase-3 inactivation and stabilization of beta-catenin induce nephron differentiation in isolated mouse and rat kidney mesenchymes. *J Am Soc Nephrol* **18**, 1130–1139.

[30] Zhang L, Chen M, Wen Q, Li Y, Wang Y, Wang Y, Qin Y, Cui X, Yang L, and Huff V, et al (2015). Reprogramming of Sertoli cells to fetal-like Leydig cells by Wt1 ablation. *Proc Natl Acad Sci U S A* **112**, 4003–4008.